IHJPAS. 35(4)2022

Ibn Al-Haitham Journal for Pure and Applied Sciences

Journal homepage: http://jih.uobaghdad.edu.iq/index.php/j/index

# Growth and Characterization of Vacuum Annealing AgCuInSe2 Thin Film

**Rana Hameed Athab**
Department of Physics, College of Education for Pure Science (Ibn-AL-Haitham),University of Baghdad, Baghdad,Iraq.
rana.hameed1104a@ihcoedu.uobaghdad.edu.iq

**Bushra H. Hussein**
Department of Physics, College of Education for Pure Science (Ibn-AL-Haitham),University of Baghdad, Baghdad,Iraq.
boshra.h.h@ihcoedu.uobaghdad.edu.iq

**Article history: Received 6 June 2022, Accepted 21 August 2022, Published in October 2022.**

**Doi: 10.30526/35.4.2868**

## Abstract

The influence of annealing on quaternary compound Ag0.9Cu0.1InSe2 (ACIS) thin film is considered a striking semiconductor for second-generation solar cells. The film deposited by thermal evaporation with a thickness of about 700 nm at R.T and vacuum annealing at temperatures (373,473) K for 1 hour. It was deposited in a vacuum of 4.5*10-5 Torr on a glass substrate. From XRD and AFM analysis, it is evident that Ag0.9Cu0.1InSe2 films are polycrystalline in nature, having ideal stoichiometric composition. Structural analysis indicated that annealing the films following the deposition resulted in the increasing polycrystalline phase with the preferred orientation along (112) direction. , increasing crystallite size and average grain size after annealing . The optical properties of these films are determined by the wavelength between 400 nm – 1000 nm. The band gap of the Ag0.9Cu0.1InSe2 films was evaluated to be (1.68-1.5) eV, and the optical constants calculated, such as the refractive index, the extinction coefficient, and the real and imaginary parts of the dielectric constant.

**Keywords**: Optical properties, AgCuInSe2, AFM, thin film.

## 1. Introduction

Ternary compounds $AgInSe_2$ and $CulnSe_2$ are direct band gap semiconductors crystallizing in the chalcopyrite structure. The nearest chemical, and electronic properties are analogues to binary zinc blende II-VI [1,2] I-III–VI2 semiconductors Group involve two metals and one chalcogen [3]. Their bandgaps lies between 0.8 and 2.0 eV [4] and between 1.07 and 2.73 eV cover the entire solar spectrum which make it an ideal system for multi-junction solar cell [5]. The crystal structure is tetragonal structure chalcopyrite with the lattice constant a =b= 6.102 A° and c = 11.69 A° of

$AgInSe_2$ and a =b= 5.781 A° and c = 11.552 A° of $CuInSe_2$ [6,7]. These thin-film semiconductor has been attractive material for solar cells because of their low production costs, high absorption, and chemical flexibility that allows for the alteration of the bandgap [8] high optical absorption coefficient, high carrier mobility, long term optoelectronic stability [9] Thin film of quaternary compound $AgCuInSe_2$ has been deposited by several methods such as pulsed laser[1] molecular beam epitaxy [10] Hybrid magnetron sputtering /evaporation[5] direct current (dc) magnetron sputtering [11] thermal evaporation [12,13] sputtered [9] The chalcogenide semiconductor family I–III–VI2 is $AgInSe_2$, and $CulnSe_2$ have suitable band-gap energies, the attention of much recent research because of their excellent electrical and optical properties, very significant application in optical devices (linear and nonlinear), photovoltaic solar cell, NIR applications in addition to the preparation of solar cells device and Schottky diode [14,15] The ionic radii of Cu doping being smaller than the ionic radius of Ag ion. Is suitable dopant for AIS lattice because the lower ionic radii $Cu^{+1}$ (0.71Å ) than Ag $^{+1}$ (1.29Å). So Cu is of great interest as a substitute for Ag, the structural, optical and electrical properties of AIS film could be controlled. [16,17]. This work concentrate on the fabrication of $AgCuInSe_2$ thin film by vacuum evaporation method and study the concentrate on the effect of annealing (473,573) K on their description using XRD, AFM, optical measurement of $AgCuInSe_2$ film and the interconnection between these parameters.

## 2. Experimental

High purity for quaternary compound Silver, Copper, Indium, and selenium ACIS elements stoichiometric is proportions by weight (0.9:0.1:1:2). Then, mix these four elements and put under the pressure of ($3*10^{-3}$ mbar) in a tube of quartz. The electric oven (1300 K) used to complete the alloy was higher than the melting temperature of $AgInSe_2$ & $CuInSe_2$ [18, 19]. They are deposited on glass substrates at R.T with 700 nm thickness for photovoltaic application. They we study the electrical, structural, and optical properties of ACIS thin films, using (E 306) thermal evaporation at R.T of $4.5*10^{-5}$ Torr. X-ray diffraction XRD and AFM has characterized the structural morphology of the ACIS films. The optical transmission measurements in the range of (400–1000) nm are done to calculate the energy gap.

X-ray diffraction has been used to study the structure of these films, and Scherer's Formula is used to calculate the crystalline size of the films [20, 21]:

$$C.S = \frac{0.9\lambda}{B cos\theta} \qquad (1)$$

where B (FWHM) is the width of the diffraction peak at half maximum intensity.

Optical properties of thin film preparation, transmission, and absorption spectrums in the wavelength range between (400 to 1000) nm have been noted, and lambert law and Tauc equation have been used to determine the absorption coefficients α and the energy gap ($Eg^{opt}$), respectively from absorption spectrum [22,23]:

$$\alpha h\upsilon = D\,(h\upsilon - E_g)^r \qquad (2)$$

$$\alpha = 2.303\frac{A}{t} \qquad (3)$$

where D is a constant that depends on the temperature and the properties of the valence & conduction bands and α: the absorption coefficient, hν the incident photon energy, r: a parameter for the type of the optical transition. A: absorbance, t: thickness.

Optical Constants such as k : extinction coefficient, n refractive index, real part $\varepsilon_r$ & imaginary part $\varepsilon_i$ of dielectric constant can be considered by the relations below[24,25,26]:

$$k = \frac{\alpha\lambda}{4\pi} \quad (4)$$

$$n = \left[\frac{4R}{(R-1)^2} - k^2\right]^{1/2} - \frac{(R+1)}{(R-1)} \quad (5)$$

$$\varepsilon_r = n^2 - k^2 \quad (6)$$

$$\varepsilon_i = 2nk \quad (7)$$

## 3. Results and Discussion

**Figure (1)** displays the XRD patterns of the deposited ACIS thin films with a thickness (700nm) at R.T and (373,473) K. The patterns show that all thin films before and after annealing have a polycrystalline with tetragonal structures. The strongest sharp peak corresponds to (112) at a diffraction angle of 25.45. All the peaks of diffraction can be assigned to the Ternary compound AgInSe2 ICDD 00-038-0952 card standard value. There is another noticeable peak (204) when diffraction angle 42.55 can observe. We can notice when annealing with temperatures (373&473), the places for measured diffraction peaks do not alter significantly, but the intensities peaks increase with annealing, and crystallite size becomes larger. This implies that crystalline films have been improved due to system regularity and reduced defects [27].

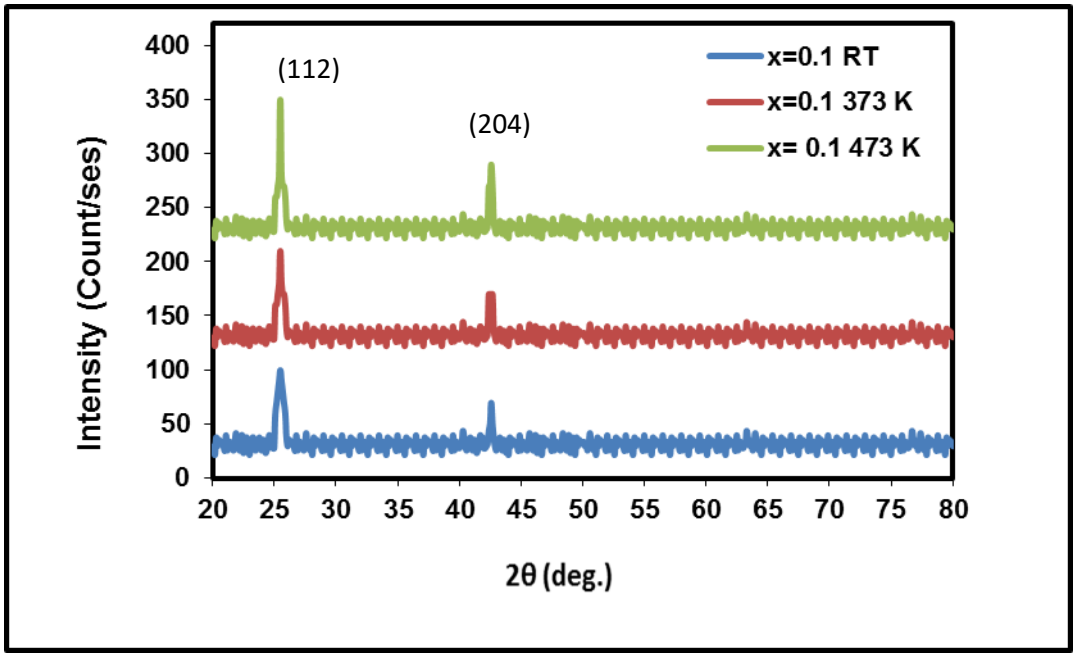


**Figure 1**. XRD pattern for thin film $Ag_{0.9}Cu_{0.1}InSe2$ at R.T and Ta(373,473) K

The crystallite size estimated by Scherer's formula is listed in **Table (1)**, showing that the sample Ag0.9Cu0.1InSe2 at 473 K has a large crystallite size from other samples. The micro strain and dislocation density were calculated, and the calculated values are given in **Table (1)**. It is evident that the micro strain δ and dislocation density ε decrease with increasing annealing temperature. This is due to the direct proportionality between the micro strain and FWHM of the main peak and the inverse proportionality between the dislocation density and the crystallite size. The decrease in Ag0.9Cu0.1InSe2 thin film defects with increasing annealing temperature indicates it improved their crystal structure.

**Table 1.** Experimental XRD data for thin films Ag0.9Cu0.1InSe2 at R.T and Ta (373,473) K

| $T_a$ (K) | $d_{exp}$ (Å) | $2\theta_{exp}$ (deg.) | hkl | FWHM (deg.) | (C.S) (nm) | $\delta*10^{15}$ (lines/$m^2$) | $\varepsilon*10^{-3}$ |
|---|---|---|---|---|---|---|---|
| R.T | 3.49 | 25.45 | 112 | 0.40000 | 21.268 | 2.2107 | 97.54 |
| | 2.12 | 42.55 | 204 | | | | |
| 373 | 3.49 | 25.45 | 112 | 0.3548 | 23.977 | 1.7393 | 86.52 |
| | 2.12 | 42.55 | 204 | | | | |
| 473 | 3.49 | 25.45 | 112 | 0.31210 | 27.258 | 1.34587 | 76.108 |
| | 2.12 | 42.55 | 204 | | | | |

The surface morphology of the Ag0.9Cu0.1InSe2 thin films at R.T and (373,473) K was examined by AFM analysis. **Figure (2)** shows these films' Granularity Cumulation Distribution chart and three-dimensional AFM images. The small particles have grown on the substrate surface, and the pyramidal morphology variations can be seen. The observed physical dimensions of the structure, such as average grain size (G.S), roughness, and root mean square, are listed in **Table (2).** The structures varied in average grain size from (63.30 to 71.33 nm) as well as the variations in the roughness and root mean square values. It is clear from this Table that the average grain size, roughness, and root mean square is increased after vacuum annealing thin film. The sample AICS has a high value at 473 K. This behavior is due to the increase of the mobility of the atoms, which causes the agglomeration of particles and of larger particles which in turn clues to a rise of the film roughness. These observations agree with XRD results.

**Table (2):** The grain size, roughness average and Root mean square of Ag0.9Cu0.1InSe2 at R.T and Ta (373,473) K

| Thickness (700nm) | Grain size (G.S) (nm) | Roughness average (nm) | r.m.s (nm) |
|---|---|---|---|
| **R.T** | 63.30 | 4.75 | 5.92 |
| **373** | 68.62 | 5.84 | 7.26 |
| **473** | 71.33 | 8.07 | 10.4 |

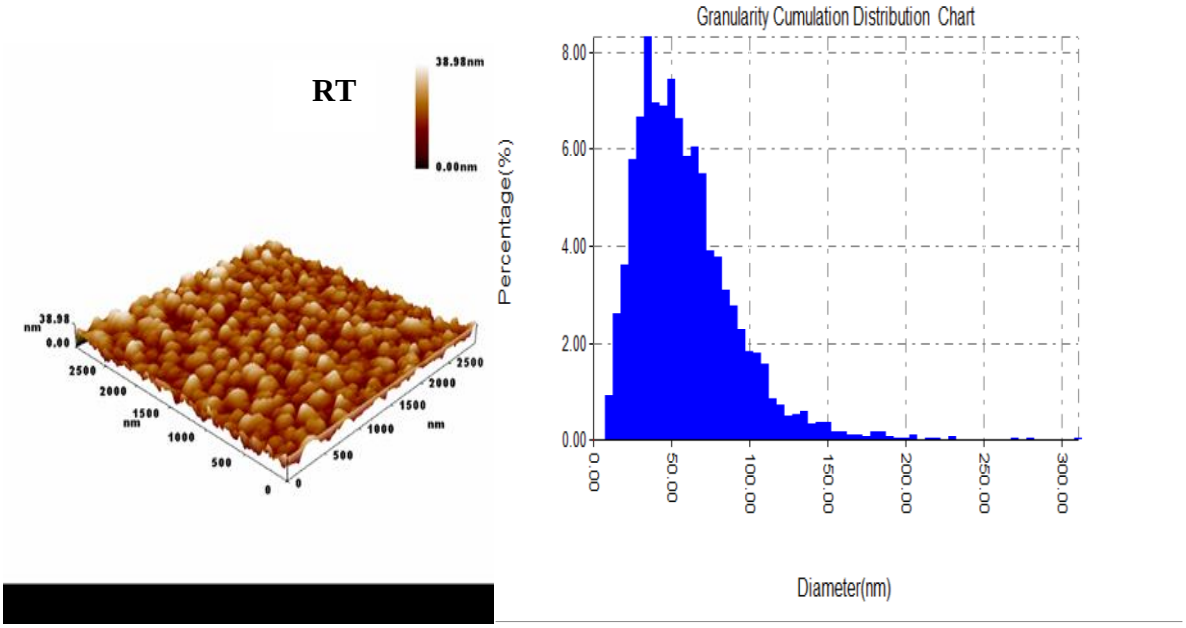


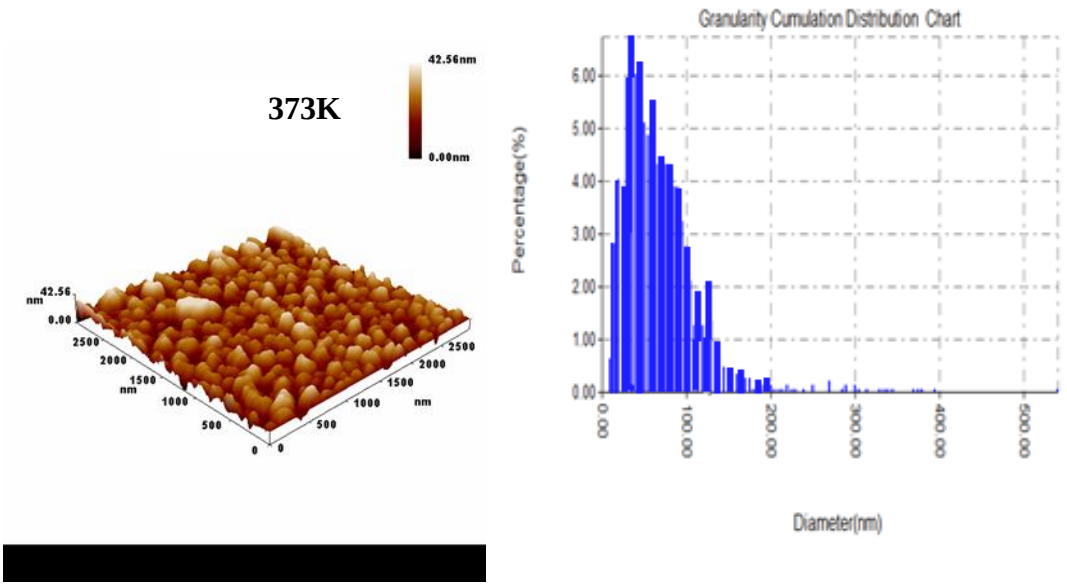

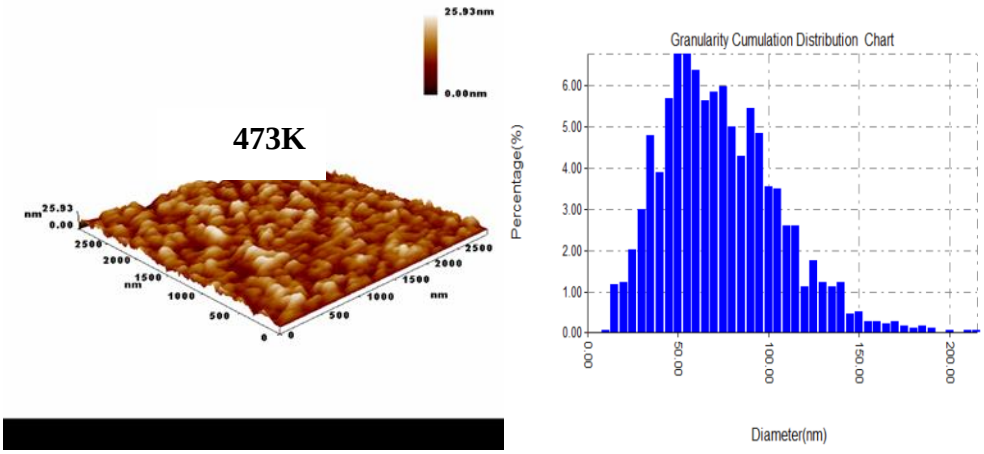


**Figure 2.** Granularity Cumulation Distribution chart and three dimension Ag0.9Cu0.1InSe2 at R.T and Ta (373,473) K.

The transmittance and absorbance spectra of the Ag0.9Cu0.1InSe2 thin films at R.T and (373,473) K in the wavelength range of (400–1000) nm are displayed in **Figure (3)**. It can be seen that the transmittance values decrease when there are increases in vacuum annealing temperatures. This means after annealing, the absorbance values for these thin films increase, and the absorption of the photon by the free carrier contributes to the decrease in optical transmittance or might be attributable to the growth of the crystallite size [28]. It is clear from figure 3 that the absorbance value of prepared Ag0.9Cu0.1InSe2 thin film after annealing is near 80%. These high values make these films a desired material for photovoltaic applications. Ag0.9Cu0.1InSe2 film at 473 K has the highest values of 90% when the range of wavelength (400-600) nm. This behavior can be related to XRD and AFM data to understand the correlation between surface morphology and the increase in absorbance [29].

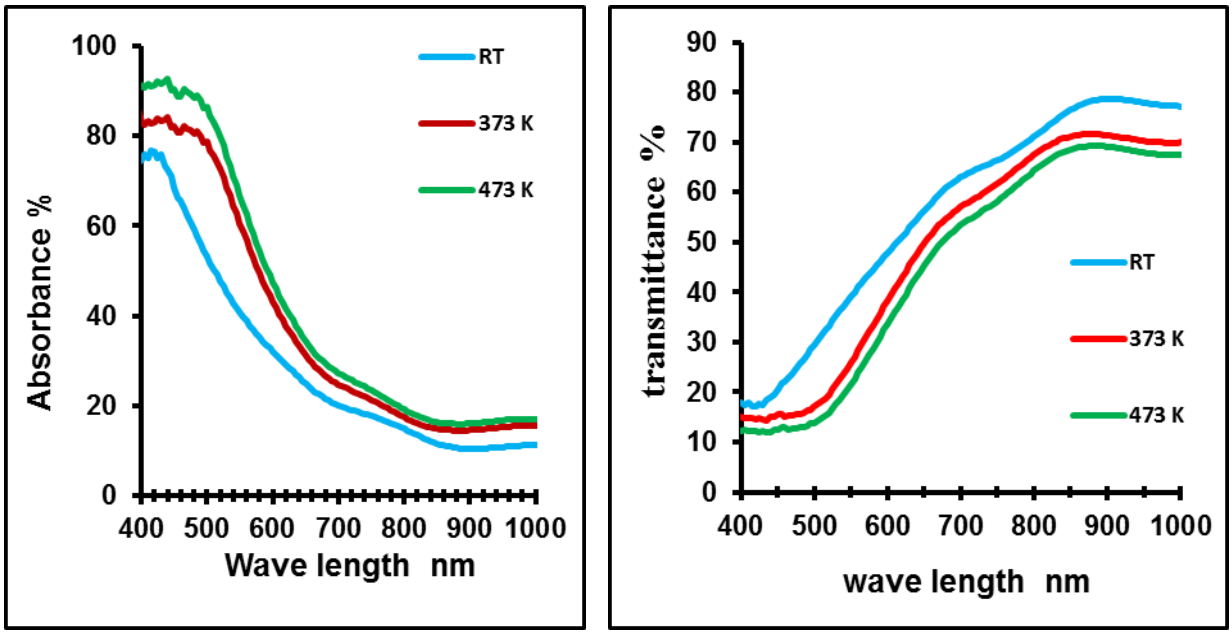


**Figure 3.** The Transmittance and Reflection spectrum of Ag0.9Cu0.1InSe2 at R.T and Ta (373,473) K

The Tauc equation was used to calculate the energy gap. It is appraised from the extrapolation to zero absorption in the Tauc equation. The variation of Eg Ag0.9Cu0.1InSe$_2$

thin films at R.T and (373,473) K is illustrated in **Figure (4)**. The allowed direct transition optical energy gaps of Ag0.9Cu0.1InSe2 films were calculate from 1.68eV to 1.5eV good agreement with [4,9,12,29]. This means it is decreased after annealing. This decreed due to the dopant atoms at the grain boundaries, and more absorbance can be obtained in Ag0.9Cu0.1InSe2. The absorption coefficient α is calculated from the exponential law, the Urbach law. In this present study, the α values before and after annealing are shown in **Table (3)**. The high value is $5.3\times10^4$ cm-1 for $Ag0.9Cu0.1InSe_2$ film at 473 K. These values indicate the increasing of localized states in the band gap after the annealing.

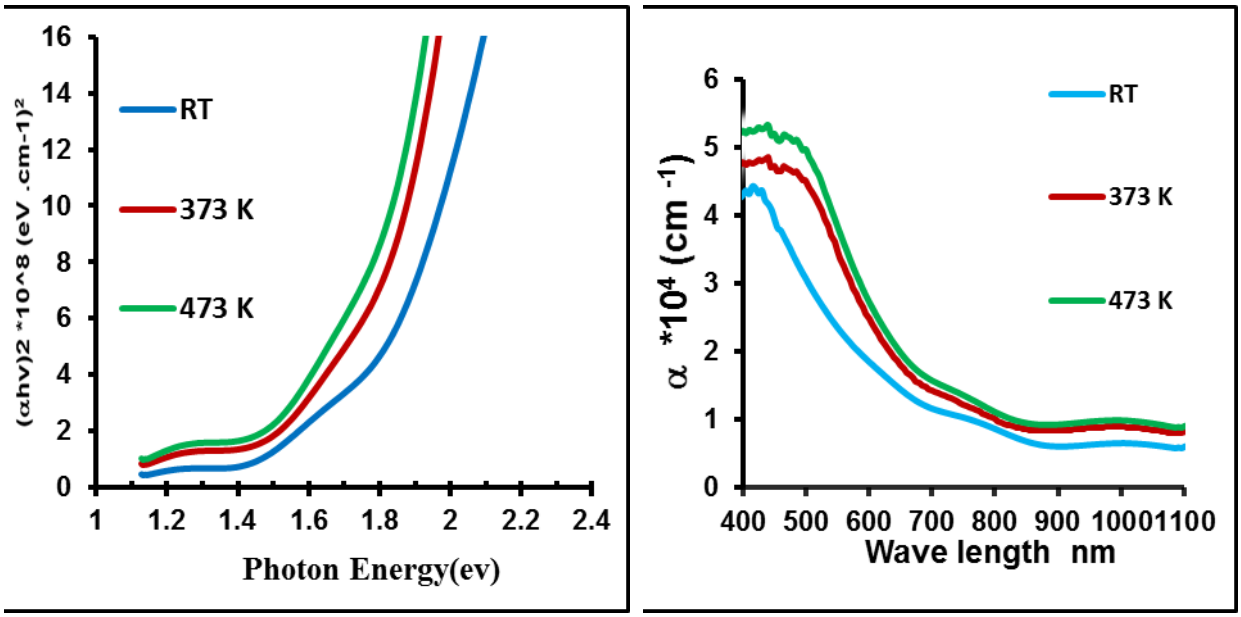


**Figure 4.** The $(\alpha h\upsilon)^2$ with photon energy $E_g$ and absorption coefficient with photon energy of $Ag_0.9Cu_0.1InSe_2$ at R.T and Ta (373,473) K.

**Table 3:** The optical parameters ($E_g^{opt}$, α, k, n, εr and εi )for $Ag_0.9Cu_0.1InSe_2$ at R.T and Ta (373,473) K. where λ=550nm

| **Thickness (700nm)** | **$E_g^{opt}$ (eV)** | **$\alpha\times10^4$ $cm^{-1}$** | **n** | **k** | **εr** | **εi** |
|---|---|---|---|---|---|---|
| R.T | 1.68 | 2.34 | 1.8 | 0.1 | 3.7 | 0.37 |
| 473 | 1.65 | 3.49 | 1.57 | 0.15 | 2.46 | 0.48 |
| 573 | 1.5 | 3.9 | 1.52 | 0.16 | 2.28 | 0.51 |

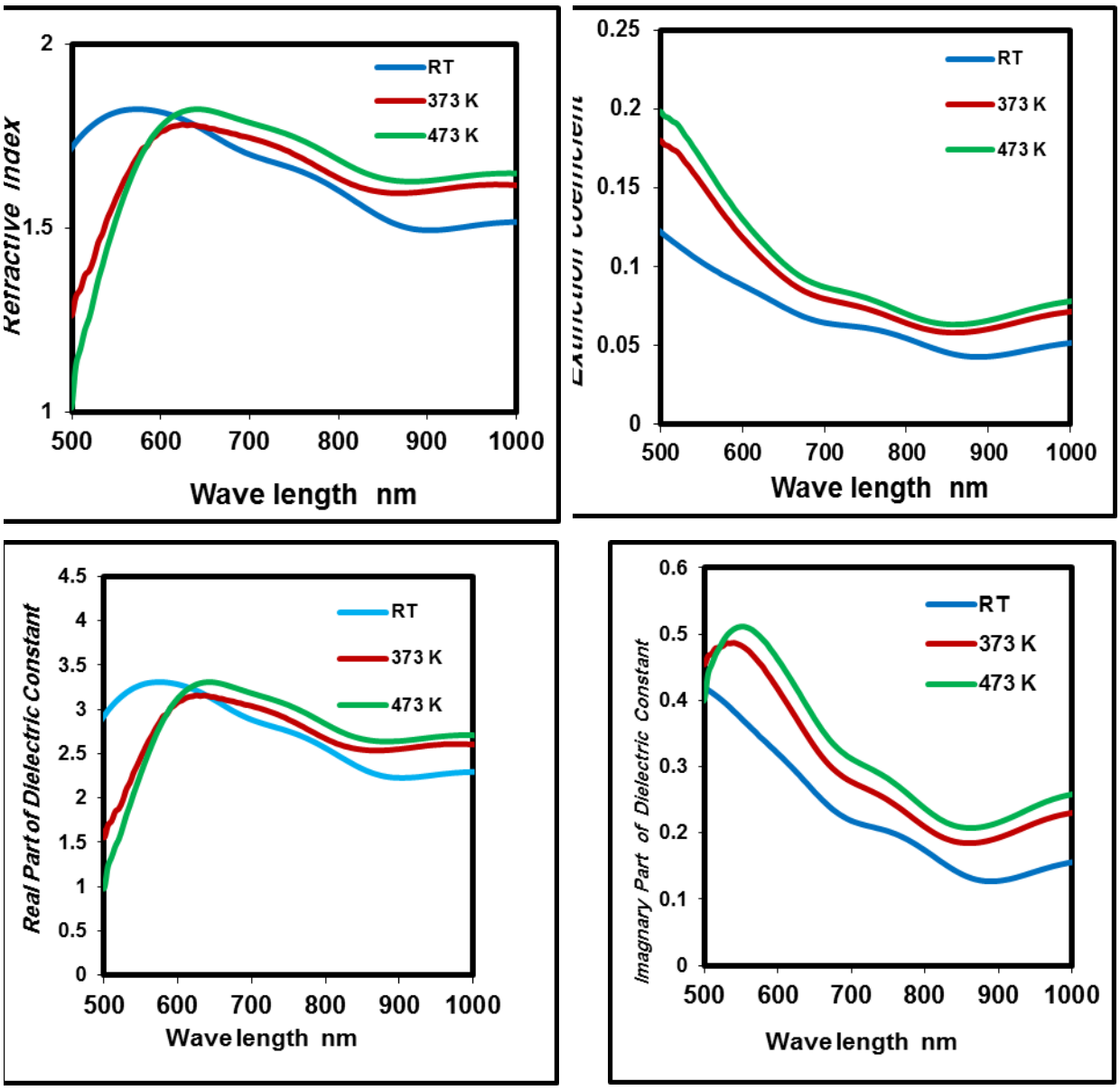


**Figure 5.** Variation of refractive index, Extinction coefficient , of the real and imaginary part of dielectric constant with wavelength for $Ag_0.9Cu_0.1InSe_2$ at R.T and Ta (373,473) K.

The value of the refractive index (n), the extinction coefficient (k), and the real and imaginary parts of the dielectric constant (εr, εi) for thin film $Ag_0.9Cu_0.1InSe_2$ at R.T and (373,473) K calculated from equations of optical constants. The calculated values of optical constant at the wavelength (λ) equal to 550nm (Within the visible range) are listed in Table (3). The refractive index n is a significant parameter for optical material and application. The values of n decrease with vacuum annealing, due to a decrease in the corresponding reflection and the structural and compositional changes with annealing. This result agrees with [1, 12]. The extinction coefficient increases, as seen in Table (3), taking the same behaviour as the absorption coefficient because the extinction coefficient is directly related to the light absorption. The fundamental electron excitation spectrum of the film was termed by means of the frequency dependency of the complex dielectric constant. The real (εr) and imaginary (εi) parts of the dielectric constant are related to the n and k values. The value of εr and εi at λ=550nm decreases because the behavior of εr is similar to that of n. In contrast, the behavior of εi is similar to that of k because it mainly depends on the k value. The

value of εi was smaller than that of the thin film at RT, which indicates a small dielectric loss. The best optical constant was when the vacuum annealing effect of 473 K.

## 4. Conclusions

Thin films of polycrystalline $Ag_0.9Cu_0.1InSe_2$ at R.T and (373,473) K with thickness of 700 nm are prepared by the thermal evaporation method. XRD and AFM studies reveal that the vacuum annealing effect $Ag_0.9Cu_0.1InSe_2$ has the strongest effects on the structural and morphology of the films. as well as the crystallite size and the average grain size increase after annealing. $Ag_0.9Cu_0.1InSe_2$ films display good absorption in the spectral range (400-700) nm. The band gap of the $Ag_0.9Cu_0.1InSe_2$ films was evaluated to be (1.68-1.5) eV. This makes it suitable for forming a solar cell junction.

**References**

1.Valery, G.; Ivan, V. B.; Ignacio, M.; Felix, L. M.; Sergeev, N.; and Victorov, I. A.; Growth and characterization of CuxAg1-xInSe2 thin films by pulsed laser Deposition, Solid State Phenomena**, 1999,** *67-68*, 361-366, https://www.researchgate.net/publication/286003594

2.Tinoco, T.; Rincón, C.; Quintero, M.; Pérez, G. S. N., *Phase Diagram and Optical Energy Gaps for* $CuIn_yGa_{1-y}Se_2$ *Alloys,* Physica Status Solidi A, **1991**, *124, 2,* 427–434,https://doi.org/10.1002/pssa.2211240206

3.Mahmoud, F. A.; and Sayed, M. H.; Preparation and Characterization OF Sprayed AgInSe2 Thin Films**,** Chalcogenide Letters, **2011**, *8, 11* , 595-600, https://chalcogen.ro/595_Mahmoud.pdf

4.Suha, N. S.; Bushra, H. H.; Influence of Al dopant on Structural and Optical Parameters of AgInSe2 thin film, Chalcogenide Letters, **2022**, *6, 19*, 409-416. https://doi.org/10.15251/CL.2022.196.409

5.Angel, R.; Aquino, A. Rockett, S.; Little, A.; and Sylvain Marsillac, Cryogenic Cathodoluminesc from CuxAg1-xInSe2 Thin Films, IEEE, **2010**, *978,* 003586 – 003590.

6.Qian, C.; Xihong, P.; and Candace K.; Structural and Photoelectrochemical Evaluation of Nanotextured Sn-Doped AgInS2 Films Prepared by Spray Pyrolysis, ChemSusChem, **2013**, *6*, 102 – 109, https://doi.org/10.1002/cssc.201200588

7.Ferhi, S.; Boujmil, M. F.; Bessaïs, B., Structural and optical modeling of electro deposited CuInSe2 thin films, EPJ WebofConferences,**2012**, *29, 00017*, 1-6, http://dx.doi.org/10.1051/epjconf/20122900017

8.Angel, R.; Aquino, S.; Little, A.; Sylvain, M.; Rob C.; and Angus, R.; Identification of Defect Levels in CuXAg1-XInSe2 Thin Films via Photoluminescence, IEEE, **2011**, *978,* 003532 – 003536.

9.Lin, R.; Zhang, T.; Hao, W. Li.; Wei, P.; Yi C.; Chen, X.; Mei Song1, Yongzhe Zhang, and Hui Yan , Structure and photoelectrochemistry of silver-copper-indium-diselenide ((AgCu)InSe2) thin film, Superlattices and Microstructures, **2017**, 114, 370-378, https://doi.org/10.1016/j.spmi.2017.12.057

10.Keiichirou, Y.; Nobuyuki, H.; Tokio, N.; Crystallographic and electrical properties of wide gap Ag(In1Kx,Gax)Se2, thin films and solar cells, Science and Technology of Advanced Materials, **2006**, *7*, 42-45, https://doi.org/10.1016/j.stam.2005.11.016

11.T. Begou, S. A.; Little, A.; Aquino, V.; Ranjan, A.; Rockett, R.; W. Collins, and S. Marsillac, In Situ and Ex Situ Characterization of (AG,CU)INSE2 thin Films, IEEE, **2011**, 000326 – 003528, **DOI:** 10.1109/PVSC.2011.6185920

12.H. H.; G¨ull¨u ˙I.; Candan E. Cos¸kun M. Parlak, Title: Investigation of Structural and Optical Parameters of Cu-Ag–In–Se Thin Films Deposited by Thermal Evaporation Method, Optik, **2015**, *126,18,* 1578-1583.

13.Hanan K. H.; Study the physical and optoelectronic Properties of Silver Gallium Indium Selenide AgGaInSe2/Si Heterojunction Solar Cell, AIP Conference Proceedings, **2018**, *1968 (1),* 020017-1–020017*,* https://doi.org/10.1063/1.5039176

14.Dingsheng, W.; Wen, Z.; Chenhui, H.; Qing, P.; and Yadong, L.; General synthesis of I–III–VI2 ternary semiconductor nanocrystals, Chemical Communications, **2008,** *22,* 2556-2558, DOI https://doi.org/10.1039/B800726H

15.Prabukanthan, P.; Sreedhar, M.; Meena, J.; Ilakiyalakshmi, M.; Venkatesan, S.; Harichandran, G.; Vilvanathaprabu, A.; and Seenuvasakumaran, P.; Influence of complexing agents-aided CuInSe2 thin films by single-step electrochemical deposition and photoelectrochemical studies, *Journal of Materials Science: Materials in Electronics*, **2021**, *32*, 6855–6865.

16.Shannon, R. D.; Acta Crystallogr A., Revised effective ionic radii and systematic studies of interatomic distances in halides and chalcogenides, **1976**, *32 (5)* 751-767, https://doi.org/10.1107/S0567739476001551

17. Greenwood N. N.; and Earnshaw, A. Chemistry of the Elements, *2nd edition Elsevier*, **1997**. ISBN: 9780750633659

18.Panda, R.; Khan, S. A.; Singh, U. P.; Naik, R.; and Mishra, N. C.; The impact of fluence dependent 120 MeV Ag swift heavy ion irradiation on the changes in structural, electronic, and optical properties of AgInSe2 nanocrystalline thin films for optoelectronic applications, RSC Adv., **2021**, *11*, 26218–26227. https://doi.org/10.1039/D1RA03409J

19.Madelung, O.; Rössler, U.; Schulz, M.; Ternary Compounds, Organic Semiconductors, Vol. III, *Springer*, **2000**, ISBN: 978-3-540-6678.

20.Khudayer, I. H.; and Hussien, B. H.; Study of Some Structural and Optical Properties of AgAlSe2 Thin Films, *Ibn Al-Haitham J. for Pure & Appl. Sci*., **2016**, *29, 2* ,41-51.

21.Bushra, K. H.; Characterization of n-CdO:Mg /p-Si Heterojunction Dependence on Annealing Temperature, *Ibn Al-Haitham J. for Pure & Appl. Sci.*,**2016**, *29 3,* 14–25.

22.Bushra, H. H.; Iman H. K.; Mohammed, H. M.; and Auday, H. S.; Effect of V, In and Cu doping on properties of p-type ZnSe/Si heterojunction solar cell An International Journal (PIE), **2019**, *13, 2,* 173-186, https://doi.org/10.1504/PIE.2019.099358

23.Bushra, K. H.; Bushra, H. H.; Hanan. K. H.; Growth and Optoelectronic Properties of p- CuO:Al/n-Si heterojunction, *Journal of Ovonic Research*, **2021**, *16 (5),* 267 - 271.

24.Bushra, H. H.; Hanan, K. H.; Bushra, K. H.; Suad. H. A.; Effect of copper on physical properties of CdO thin films and n-CdO: *Cu / p-Si heterojunction Journal of Ovonic Research*, **2022,** *18 (1)*, 37-41, https://doi.org/10.15251/JOR.2022.181.37

25.Sze, S.; and Ng., K.; *Physics of Semiconductor Devices*, 3rd edition, *John Wiley and Sons*, **2007**, ISBN:9780470068328, https://doi.org/10.1002/0470068329

26.Schroder, D.; Semiconductor Material and Device Characterization, 3rd edition, *John Wiley& Sons*, **2006**, ISBN:9780471749097, https://doi.org/10.1002/0471749095

27.Wadaa, S. H.; Ala' Fadhil A.; Kadhim, A. A.; Influence of Laser Energy and Annealing on Structural and Optical Properties of CdS Films Prepared by Laser Induced Plasma, , *Iraqi Journal of Science*, **2020**, *61, 6,* 1307-1312, DOI:10.24996/ijs.2020.61.6.8

28.Tigau, N.; Ciupina, V.; Prodan, G.; Rusu, G. I.; Gheorghies, C.; Vasile, E.; The influence of heat treatment on the electrical conductivity of antimony trioxide thin films, *Journal of Optoelectronics and Advanced Materials*, **2003,** *5, 4,* 907-912.

29.Kihwan, K.; Seung, K. A.; Jang, H. C.; Jinsoo, Y.; Young, J. E.; Jun, S. C.; Ara, C.; Jihye, G.; Soomin, S.; Dae, H. C.; Yong, D. C.; Jae, H. Y.; Highly Efficient Ag-Alloyed Cu(In,Ga)Se2 Solar Cells with Wide Bandgaps and Their Application to Chalcopyrite-Based Tandem Solar Cells, Nano Energy, **2018,** *48*, 345-352.